ACADEMIC PRESS

Archives of Biochemistry and Biophysics 403 (2002) 121–131

ABB

www.academicpress.com

Allosterically linked noncompetitive antagonist binding sites in the resting nicotinic acetylcholine receptor ion channel

Hugo R. Arias,[a] Elizabeth A. McCardy,[b] Erin Z. Bayer,[b] Martin J. Gallagher,[c] and Michael P. Blanton[b,*]

[a] *Department of Pharmacology and Therapeutics, College of Medicine, University of Florida, Gainesville, FL, USA*
[b] *Departments of Pharmacology and Anesthesiology, School of Medicine, Texas Tech University Health Sciences Center, 3601 4th Street, Lubbock, TX 79430, USA*
[c] *Department of Neurology, Washington University School of Medicine, St. Louis, Missouri, USA*

Received 21 March 2002, and in revised form 29 April 2002

Abstract

Previous studies have established the presence of overlapping binding sites for the noncompetitive antagonists (NCAs) amobarbital, tetracaine, and 3-trifluoromethyl-3-(*m*-[^{125}I]iodophenyl) diazirine ([^{125}I]TID) within the ion channel of the *Torpedo* nicotinic acetylcholine receptor (AChR) in the resting state. These well-characterized NCAs and competitive radioligand binding and photolabeling experiments were employed to better characterize the interaction of the dissociative anesthetics ketamine and thienylcycloexylpiperidine (TCP) with the resting AChR. Our experiments yielded what appear to be conflicting results: (i) both ketamine and TCP potentiated [^{125}I]TID photoincorporation into AChR subunits; and (ii) ketamine and TCP had very little effect on [^{14}C]amobarbital binding. Nevertheless, (iii) both ketamine and TCP completely displaced [^{3}H]tetracaine binding (K_is $\sim$ 20.9 and 2.0 μM, respectively) by a mutually exclusive mechanism. To reconcile these results we propose that, in the resting ion channel, TCP and ketamine bind to a site that is spatially distinct from the TID and barbiturate locus, while tetracaine bridges both binding sites.

Keywords: *Torpedo* nicotinic acetylcholine receptor; Equilibrium binding; Photoaffinity labeling; Ketamine and phencyclidine binding sites; Conformational states

The muscle-type nicotinic acetylcholine receptor (AChR)[1] isolated from *Torpedo californica* electric organs has been studied extensively over the past several decades and serves as the archetype of a ligand-gated ion channel superfamily. This genetically linked receptor superfamily includes both muscle- and neuronal-type AChRs, type A and C γ-aminobutyric acid, type 3 5-hydroxytryptamine, and glycine receptors (reviewed in [1,2]). Each of these structurally and functionally homologous receptors exists in at least three interconvertible conformational states: the resting (closed) state (in the absence of agonist), the open state (in the presence of agonist), and the desensitized (closed) state (in the prolonged presence of agonist) (reviewed in [1,3]).

The functional response of each of these receptors can be inhibited by two main pharmacological mechanisms: a competitive (e.g., a ligand that competes for the same neurotransmitter binding site) and a noncompetitive mechanism [e.g., a drug that does not compete for the neurotransmitter binding site but binds to other inhibitory site(s)]. For example, agonist-induced activation of the *Torpedo* AChR is competitively inhibited by

* Corresponding author. Fax: +1-806-743-2744.
E-mail address: michael.blanton@ttmc.ttuhsc.edu (M.P. Blanton).

[1] *Abbreviations used:* AChR, nicotinic acetylcholine receptor; carb, carbamylcholine; NCA, noncompetitive antagonist; PCP, phencyclidine; TCP, thienylcyclohexylpiperidine; [^{3}H]TCP, [piperidyl-3,4-^{3}H(*N*)]-(*N*-(1-(2-thienyl)cyclohexyl)-3,4-piperidine; [^{125}I]TID, 3-trifluoromethyl-3-(*m*-[^{125}I]iodophenyl) diazirine; amobarbital, 5-ethyl-5′-(3-methylbutyl) barbituric acid; VDB, vesicle dialysis buffer; IC_{50}, competitor concentration that inhibits 50% drug maximal binding to the AChR; EC_{50}, modulator concentration that enhances 50% drug activity (e.g., binding or photoincorporation) on the AChR; K_i, inhibition constant; K_d, dissociation constant; n_H, Hill coefficient; Mops, 4-morpholinpropanesulfonic acid; RT, room temperature; SDS–PAGE, sodium dodecyl sulfate–polyacrylamide gel electrophoresis.

0003-9861/02/$ - see front matter
PII: S0003-9861(02)00214-X

α-bungarotoxin and *d*-tubocurarine (reviewed in [1,3]) and noncompetitively inhibited by compounds referred to as noncompetitive antagonists (NCAs) (reviewed in [3,4]). NCAs of the AChR represent a structurally diverse group of compounds that include local anesthetics, phencyclidine (PCP), steroids, and even the neuropeptide substance P. Therefore, inhibition of receptor function likely occurs via several different mechanisms. Some NCAs may inhibit the AChR by simply binding within the pore of the ion channel when the receptor is in the open state, physically blocking the permeation of ions (e.g., open-channel-blocking mechanism). Other NCAs may inhibit receptor function by preferentially binding to and stabilizing a nonconducting conformational state of the AChR (e.g., resting, desensitized state; allosteric mechanisms). Further, it is likely that many NCAs inhibit receptor function by utilizing more than one mechanism of inhibition.

Examples of NCAs that likely inhibit AChR function by binding with high affinity to the AChR in the resting state include tetracaine, barbiturates, and 3-trifluoromethyl-3-(*m*-[^{125}I]iodophenyl)diazirine ([^{125}I]TID) [5–8]. For TID [9,10] and tetracaine [11], photoaffinity labeling and biochemical studies have identified their respective binding sites within the ion channel of the AChR resting state. The TID site is located approximately in the middle of each channel-lining M2 segment, more specifically between the highly conserved ring of leucine residues (M2–9; e.g., δLeu^{265}) and the more extracellular ring of valine residues (M2–13; e.g., δVal^{269}). The tetracaine binding site overlaps the TID site (M2–9 and M2–13), but includes additional residues (e.g., α1Ile^{247}, M2-5, and δAla^{268}, M2–12) [11], indicating that the tetracaine binding site encompasses a greater span of the resting channel. A combination of competitive binding and photolabeling experiments has demonstrated that the high-affinity barbiturate binding site overlaps that for tetracaine and TID [8].

While the binding sites for tetracaine, TID, and barbiturates overlap, it does not appear as if there is just a single NCA binding site on the resting AChR. For example, the dissociative anesthetic PCP, a well-characterized NCA that binds with high affinity to both the resting and the desensitized AChR [12], interacts allosterically with TID and apparently competitively with tetracaine [13,14]. Ketamine, another dissociative anesthetic and a congener of PCP, is also a NCA of the AChR, inhibiting the open channel of both muscle- [15–17] and neuronal-type AChRs [18–21], as well as closed (resting) ion channels [16]. Further, ketamine completely displaces [^{3}H]PCP binding to the *Torpedo* AChR in either the resting or the desensitized state [17,22]. Lastly, thienylcycloexylpiperidine (TCP), a close structural analog of PCP, binds to desensitized *Torpedo* AChRs with nearly identical affinity as PCP [23,24]. While it is therefore clear that there exists a dissociative anesthetic binding site(s) on the resting AChR, there is little or conflicting experimental evidence regarding the localization of this site(s) [13].

To characterize and possibly identify the binding site for ketamine and TCP (as well as PCP) on the resting AChR, we employed competitive radioligand binding and photolabeling experiments using well-characterized NCAs (e.g., tetracaine, TID, and amobarbital). More specifically, we tested the ability of ketamine, the *S*(+) enantiomer of ketamine alone, as well as TCP and tetracaine, to affect either the photoincorporation of [^{125}I]TID or the binding of [^{14}C]amobarbital, [^{3}H]tetracaine, or [^{3}H]TCP to the receptor in the resting state. We wished to characterize the interaction between the binding of each of these ligands as well as the nature of the interaction, i.e., allosteric or competitive (steric).

Materials and methods

Materials. [Piperidyl-3,4-^{3}H(*N*)]-(*N*-(1-(2-thienyl)cyclohexyl)-3,4-piperidine) ([^{3}H]TCP; 57.6 Ci/mmol) was obtained from New England Nuclear Research Products (Boston, MA), 3-trifluoromethyl-3-(*m*-[^{125}I]iodophenyl)diazirine ([^{125}I]TID; ~10 Ci/mmol) from Amersham Pharmacia Biotech (Piscataway, NJ), and both were stored in ethanol at −20 and 4 °C, respectively. [^{3}H]Tetracaine (36 Ci/mmol) was a gift from Dr. Jonathan Cohen (Harvard Medical School, Boston, MA), [^{14}C]amobarbital (50 mCi/mmol) was synthesized by American Radiolabeled Chemicals (St. Louis, MO), and both were stored in ethanol at −20 °C. Suberyldicholine dichloride, carbamylcholine chloride (carb), proadifen hydrochloride, amobarbital hydrochloride, tetracaine hydrochloride, ketamine hydrochloride, *S*(+)-ketamine hydrochloride, phencyclidine hydrochloride, and thienylcyclohexylpiperidine hydrochloride were all purchased from Sigma Chemical [1-(Dimethylamino) napthalene-5-sulfonamido]ethyltrimethylammonium perchlorate (dansyltrimethylamine) was obtained from Pierce Chemical (Rockford, IL). *Staphylococcus aureus* V8 protease was purchased from ICN Biochemicals (Costa Mesa, CA). Other organic chemicals were of the highest purity available.

Preparation of AChR native membranes. AChR native membranes were prepared from frozen *T. californica* electric organs obtained from Aquatic Research Consultants (San Pedro, CA) by differential and sucrose density gradient centrifugation, as described previously [25]. The specific activities of these membrane preparations were determined by the decrease in dansyltrimethylamine (6.6 μM) fluorescence produced by the titration of suberyldicholine into receptor suspensions (0.3 mg/ml) in the presence of 100 μM PCP and ranged from 0.9 to 1.2 nmol of suberyldicholine binding sites/mg total protein (0.45–0.60 nmol AChR/mg protein).

Dansyltrimethylamine excitation and emission wavelengths were 280 and 546 nm, respectively. To reduce stray-light effects a 530-nm cutoff filter was placed in the path of the dansyltrimethylamine emission beam. The AChR membrane preparations (in ~36% sucrose, 0.02% NaN_3) were stored at −80 °C.

Effect of ketamine and TCP on [^{125}I] TID photoincorporation into the resting AChR. To determine the effect of ketamine (racemic mixture), the *S*(+) enantiomer of ketamine, and TCP on [^{125}I]TID photoincorporation into the AChR, 0.2 μM AChR native membranes were suspended in 8 ml of vesicle dialysis buffer (VDB; 10 mM Mops, 100 mM NaCl, 0.1 mM EDTA, and 0.02% NaN_3, pH 7.5), with ~430 nM [^{125}I]TID, in the absence of carbamylcholine (carb) (i.e., resting state). The total volume was then divided into aliquots, and increasing concentrations of ketamine, *S*(+)-ketamine, or TCP (1–120 μM) were added from ethanolic stock solutions (ethanol concentration <1%) to each tube and the membrane suspension was allowed to incubate for 1 h at room temperature (RT). Membranes were then irradiated for 7 min at a distance of <1 cm with a 365-nm lamp (Spectroline Model EN-280L; Spectronics, Westbury, NY) and labeled polypeptides separated by SDS–PAGE [10,13]. After electrophoresis, the polypeptides in the polyacrylamide gel were visualized by Coomassie blue stain and following autoradiographic analysis of the dried gel [10], the gel band for each AChR subunit was excised and the amount of ^{125}I-cpm measured with a Packard Cobra II gamma counter. Nonspecific photoincorporation was determined in the presence of 0.4 mM carb as described previously [10].

Proteolytic mapping of the sites of [^{125}I]TID photoincorporation within AChR subunits was performed according to the method of Cleveland et al. [26] and as described in detail in Blanton et al. [27]. Briefly, the gel containing the AChR subunits photolabeled with [^{125}I]TID was soaked in water overnight. The AChR α-subunit bands were excised and the gel pieces soaked in overlay buffer [5% (w/v) sucrose, 125 mM Tris–HCl, 0.1% (w/v) SDS, pH 6.8] for 20 min [26]. The gel pieces were then transferred to the wells of a 15% acrylamide mapping gel and overlaid with 15 μl of 0.4 μg/μl *S. aureus* V8 protease (~6 μg α-subunit; 6 μg V8 protease). Following electrophoresis, gels were stained, destained, dried, and exposed to Kodak X-OMAT LS sensitive films with an intensifying screen at −80°C for several days. The amount of [^{125}I]TID photoincorporation into AChR α-subunit V8 protease fragments was determined by gamma counting of excised gel bands.

Effect of amobarbital, tetracaine, and ketamine on [^{3}H]TCP, [^{3}H]tetracaine, or [^{14}C]amobarbital binding to the AChR. The effect of amobarbital, tetracaine, and ketamine on [^{3}H]TCP, [^{3}H]tetracaine, or [^{14}C]amobarbital binding to the resting AChR was examined. AChR native membranes were suspended in 8 ml of VDB buffer (0.2 μM AChR) with 7.5 μM [^{14}C]amobarbital, 6.4 nM [^{3}H]TCP, or 6.9 nM [^{3}H]tetracaine, in the absence of carb (resting state), and increasing concentrations of the drug under study (0.01–200 μM). Nonspecific binding was determined in the presence of 100 μM tetracaine, or alternatively in the presence of 200 μM amobarbital. After centrifugation of the samples in a Beckman J2-HS centrifuge (Beckman Coulter, Fullerton, CA) using a JA-20 rotor (18,000 rpm for 1 h), the ^{14}C- or ^{3}H-containing pellets were resuspended in 100 μl 10% SDS and transferred to a scintillation vial with 3–5 ml Bio-Safe II (Research Products International, Mount Prospect, IL). The bound fraction was determined by scintillation counting.

For ketamine-induced inhibition of [^{3}H]TCP binding experiments in the desensitized AChR, the same protocol as in the resting state was used but in the presence of 200 μM carb to desensitize the AChR, and 200 μM proadifen to determine nonspecific [^{3}H]TCP binding.

Data analysis. For the binding experiments described above, the concentration–response data were curve-fitted by nonlinear least-squares analysis using the program Prism (GraphPad) and the corresponding EC_{50} (potentiation) and IC_{50} (inhibition) values calculated. The EC_{50} values as well as the Hill coefficient (n_H) values are summarized in Table 1. Taking into account that the resting AChR presents a single high-affinity binding site for amobarbital [8], tetracaine [5], and TCP (this paper), the observed IC_{50} values from the inhibition of radiolabeled ligand binding experiments were transformed into K_i values using the Cheng–Prusoff relationship [28],

$$K_i = IC_{50}/\{1 + ([NCA]/K_d^{NCA})\}, \quad (1)$$

where [NCA] is the initial concentration of the labeled NCA ([^{14}C]amobarbital, [^{3}H]tetracaine, or [^{3}H]TCP) and K_d^{NCA} is the dissociation constant for [^{14}C]amobarbital (3.7 μM; [8]), [^{3}H]tetracaine (0.5 μM; [5]), and [^{3}H]TCP (0.83 μM; Arias, Trudell, Bayer, Hester, McCardy, and Blanton, in preparation). The calculated K_is and n_Hs are summarized in Tables 1 and 2, respectively. The observed K_d of [^{3}H]TCP in the resting state (~0.83 μM) is about 4-fold higher than reported K_d values in the desensitized state (~0.2 μM [23]; ~0.25 μM [24]), consistent with a preference for the desensitized AChR.

In order to have a better indication whether ketamine inhibits [^{3}H]tetracaine binding to the resting AChR by a competitive (steric) or allosteric mechanism, ketamine-induced inhibition of [^{3}H]tetracaine binding experiments at increasing initial concentrations (from 6.9 to 4970 nM) of [^{3}H]tetracaine (+ unlabeled tetracaine) were performed. The rationale of this experiment is based on that, for a higher initial concentration of an AChR-bound ligand we will need a higher concentration of the competitor to produce a total ligand binding inhibition. This is consistent with Schild-type analysis [29]. From these

Table 1
Modulation of [^{125}I]TID photoincorporation as well as [^{14}C]amobarbital and [^{3}H]TCP binding by ketamine, TCP, and amobarbital to the AChR in the resting state

Method	Subunit	Modulator	$EC_{50}(K_i)$ (μM)	n_H	Figure
Ligand-induced modulation of [^{125}I]TID photoincorporation	α	Racemic ketamine	18.7 ± 7.4	2.3 ± 1.4	1
		S(+)-Ketamine	9.7 ± 2.2	1.2 ± 0.3	1
	αV8–20	Racemic ketamine	9.9 ± 2.2	0.93 ± 0.17	2
	αV8–10	Racemic ketamine	No effect	–	2
	β	Racemic ketamine	15.2 ± 3.6	2.3 ± 1.0	1
		S(+)-Ketamine	7.4 ± 4.5	4.9 ± 2.8	1
	γ	Racemic ketamine	20.4 ± 10.1	2.6 ± 1.5	1
		S(+)-Ketamine	6.6 ± 2.9	2.4 ± 1.8	1
	δ	Racemic ketamine	19.4 ± 6.5	2.4 ± 1.3	1
		S(+)-Ketamine	8.5 ± 2.4	2.0 ± 1.1	1
		TCP	1.9 ± 0.7	1.00 ± 0.36	3
Ligand-induced modulation of [^{14}C]amobarbital binding	All	Racemic ketamine	No effect	–	4
		S(+)-Ketamine	(430 ± 330)	0.32 ± 0.11	4
		TCP	(5100 ± 3600)	0.22 ± 0.04	5
Ligand-induced modulation of [^{3}H]TCP binding	All	Amobarbital	(3700 ± 2100)	0.51 ± 0.11	5

Note. EC_{50} values were calculated by nonlinear least-squares fit. Values between parentheses are apparent K_i values and were calculated using Eq. (1).

Table 2
Inhibition of [^{3}H]tetracaine and [^{3}H]TCP binding by ketamine, TCP, and tetracaine

Method	Inhibitor	K_i (μM)	n_H	Figure
Ligand-induced inhibition of [^{3}H]tetracaine binding	Racemic ketamine	20.9 ± 3.0	0.90 ± 0.08	6
	S(+)-Ketamine	19.9 ± 2.8	0.90 ± 0.09	6
	TCP	2.0 ± 0.4	0.92 ± 0.03	7
Ligand-induced inhibition of [^{3}H]TCP binding	Tetracaine	0.74 ± 0.04	1.04 ± 0.06	7
	Racemic ketamine (resting)	16.5 ± 0.7	0.92 ± 0.04	8A
	S(+)-Ketamine (resting)	18.2 ± 1.2	0.93 ± 0.05	8A
	Racemic ketamine (desensitized)	13.1 ± 1.8	0.99 ± 0.12	8B
	S(+)-Ketamine (desensitized)	15.4 ± 2.3	0.91 ± 0.11	8B

Note. K_i values were calculated using the observed IC_{50}s according to Eq. (1).

competition curves we calculated the apparent IC_{50} values. Then, we plot the ratio of IC_{50} values for ketamine determined at different initial concentrations of [^{3}H]tetracaine and 6.9 nM [^{3}H]tetracaine versus the initial tetracaine concentration: $([IC_{50}(\text{ketamine})^{\text{tetracaine}}/IC_{50}(\text{ketamine})^{\text{control}}]$ versus $[\text{tetracaine}]_{\text{initial}}$). The data points are very well fitted ($r^2 = 0.91$) by linear regression. A linear relationship is indicative of competitive interactions, whereas a nonlinear relationship suggests an allosteric mechanism of inhibition. However, the existence of a very strong allosteric inhibitory interaction between ketamine and tetracaine cannot be ruled out. In order to improve the degree of confidence of this relationship, a broad range of tetracaine initial concentrations (above the tetracaine K_d) was tested. Nevertheless, experiments with initial concentrations of [^{3}H]tetracaine (+ unlabeled tetracaine) higher than 5 μM give lower signal/noise ratios, impeding the use of the whole range of ligand concentrations.

Results

Potentiation of [^{125}I]TID photoincorporation into the resting AChR by ketamine and TCP

Because the interaction of 3-trifluoromethyl-3-(*m*-[^{125}I]iodophenyl) diazirine with the resting AChR has been very well characterized, including identification of a high-affinity binding site within the ion channel pore [9] (reviewed in [2,4]), we began our studies by examining the effect of ketamine and TCP on [^{125}I]TID photoincorporation into the resting receptor. AChR native membranes, in the absence of agonist, were equilibrated with ~430 nM [^{125}I]TID and various concentrations of ketamine, *S*(+)-ketamine, or TCP. Following photolysis the labeled polypeptides were separated by SDS–PAGE and the extent of [^{125}I]TID incorporation was assessed by both autoradiography (Fig. 1A) and by gamma counting of excised AChR subunit bands. Consistent

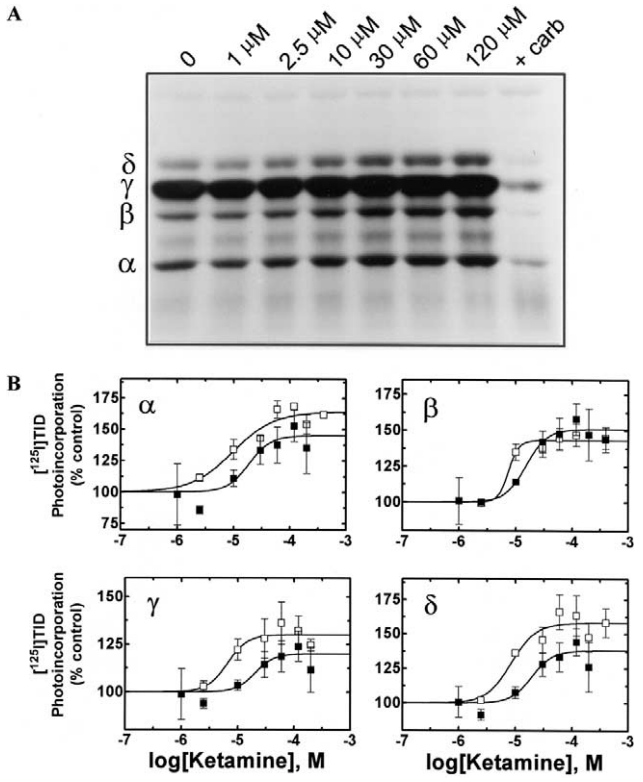

Fig. 1. Potentiation of [^{125}I]TID photoincorporation into each AChR subunit in the resting state by ketamine. (A) AChR native membranes were equilibrated (1 h) with [^{125}I]TID (430 nM) in the absence (lanes 1–7) and in the presence of 0.4 mM carb (lane 8), or in the presence of increasing concentrations of ketamine (lanes 2–7). AChR native membranes were then irradiated at 365 nm for 7 min, and polypeptides resolved by SDS–PAGE. Shown is the corresponding autoradiograph of the gel containing the concentration–response photolabeling experiments for [^{125}I]TID versus ketamine. The positions of the AChR subunits are indicated on the left. The amount of [^{125}I]TID incorporation into each AChR subunit in the presence of agonist defines the level of nonspecific labeling. (B) For each concentration of racemic ketamine (■) or *S*(+)-ketamine (□), individual AChR subunit bands were excised from the dried gel and the amount of [^{125}I]TID photoincorporated into each subunit was determined by gamma counting. The amount of [^{125}I]TID subunit incorporation determined for each concentration of ketamine or *S*(+)-ketamine is expressed as a percentage of the [^{125}I]TID subunit incorporation detected in the absence of any ligand. The concentration-dependent increase in [^{125}I]TID incorporation into each subunit was curve-fitted using nonlinear least squares. The resulting EC_{50} values are summarized in Table 1.

with previous results [10,13], [^{125}I]TID was photoincorporated into each AChR subunit, with the γ-subunit labeled ~4-fold greater than each of the other receptor subunits (Fig. 1A, lane 1). Somewhat surprisingly, ketamine, both the racemic mixture and the *S*(+) enantiomer alone, increased the extent (i.e., potentiated) of [^{125}I]TID photoincorporation into each AChR subunit in a concentration-dependent fashion (Fig. 1). The calculated EC_{50} values range from 15 to 20 μM (for racemic ketamine) and from 7 to 10 μM [for *S*(+)-ketamine] (Table 1). Since racemic ketamine is a 50:50 mix of the two stereoisomers, the *S*(+) enantiomer is 2–3 times more potent than the racemic mix. Nevertheless, the standard deviation of the EC_{50} values indicate that this is true only for the potentiation seen on the γ- and δ-subunits. These data suggest that the *S*(+) stereoisomer is the only active one, that its affinity is much greater than that of the *R*(−) enantiomer, or that it affects the binding orientation of [^{125}I]TID to a higher extent than the *R*(−) enantiomer. The *S*(+) enantiomer appears to also have a slightly greater efficacy compared to the racemic mixture. For example, for [^{125}I]TID incorporation into the δ-subunit (Fig. 1B) potentiation by *S*(+)-ketamine saturates at ~160% of the control level, while the value for the racemic mixture is ~138%. However, taking into account the standard deviations (~20–30%), this difference can be considered not statistically significant. That ketamine increases the extent of [^{125}I]TID photoincorporation into the AChR suggests an allosteric mode of interaction.

Because the vast majority (>75%) of [^{125}I]TID photoincorporation into each AChR subunit (labeled in the resting state) reflects incorporation into specific amino acids in the channel-lining M2 segment [9,10], the presumption is that the potentiation of labeling by ketamine reflects increased [^{125}I]TID labeling of the resting ion channel. This conclusion is supported by the fact that potentiation of [^{125}I]TID incorporation into the AChR δ-subunit by PCP, a congener of ketamine, is the result of increased labeling of a single residue, δLeu^{265} (i.e., position M2–9) within the δM2 segment [13]. Nonetheless, it is possible that ketamine interaction with the AChR instead results in an increase in nonspecific [^{125}I]TID photoincorporation into the AChR, perhaps at the lipid-protein interface [30,31]. To resolve this issue we mapped the [^{125}I]TID photoincorporation into the AChR α-subunit. [^{125}I]TID-labeled α-subunit was digested with *S. aureus* V8 protease, the labeled fragments were separated by SDS–PAGE, and the distribution of [^{125}I]TID labeling was assessed by both autoradiography and by gamma counting of excised V8 protease fragment bands. As shown in Fig. 2A, two labeled fragments were detected, the αV8–10 fragment (Asn^{339}–Gly^{437}) which bears the M4 transmembrane domain and the αV8–20 fragment (Ser^{173}–Glu^{338}) that contains the M1–M3 transmembrane domains. Only the αV8–20 fragment displayed increased [^{125}I]TID labeling in the presence of ketamine (Fig. 2). This demonstrates that ketamine interaction with the AChR predominantly effects [^{125}I]TID labeling of the resting ion channel.

In addition, we determined that TCP, in a fashion nearly identical to that of PCP [13,14], potentiates [^{125}I]TID photoincorporation into the δ-subunit of the AChR in a concentration-dependent fashion (only labeling in the δ-subunit is significantly affected; Fig. 3). The EC_{50} value for the δ-subunit (1.9 μM) is reported in Table 1. Again, a result showing potentiation of [^{125}I]TID photoincorporation argues strongly for an

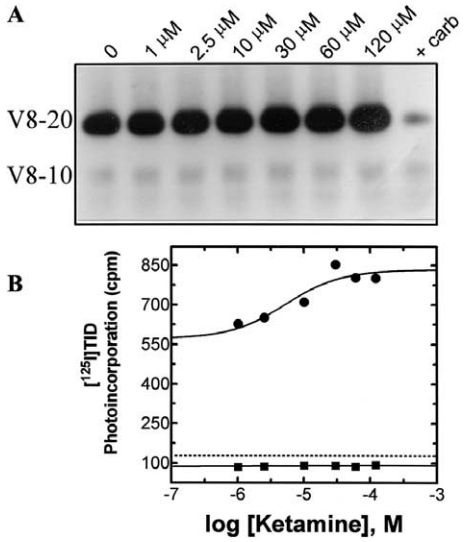

Fig. 2. Mapping the ketamine-induced potentiation of [^{125}I]TID photoincorporation to the α V8–20 fragment. (A) AChR native membranes were photolabeled with [^{125}I]TID (430 nM) in the absence (lanes 1–7) and in the presence of carb (lane 8), and in the presence of (lanes 2–7) of increasing concentrations of ketamine. Bands containing [^{125}I]TID-labeled α-subunit were excised and digested "in-gel" with *S. aureus* V8 protease (see Materials and methods). Two labeled fragments were detected (αV8–20 and αV8–10) following electrophoresis and autoradiographic analysis. The positions of the two labeled fragments are indicated on the left. (B) The extent of [^{125}I]TID incorporation into the fragment αV8–20 (●), containing the M1–M3 transmembrane domains, was found to be sensitive to the addition of ketamine, whereas the incorporation into fragment αV8–10 (■) which contains the M4 transmembrane domain was insensitive to the addition of ketamine. The dashed line shows the level of [^{125}I]TID incorporation into αV8–20 when the AChR was labeled in the presence of carb (i.e., desensitized state). The EC_{50} value (9.9 μM) for ketamine potentiation of [^{125}I]TID incorporation into αV8–20 was calculated by nonlinear least-squares analysis and the results are summarized in Table 1.

allosteric interaction between [^{125}I]TID and TCP, and that neither the ketamine nor the TCP binding site spatially overlaps the TID binding locus.

Slight inhibition of [^{14}C]amobarbital binding by ketamine and TCP, and of [^{3}H]TCP binding by amobarbital in the resting state

We next set out to exclude the possibility that the allosteric interaction between ketamine (or TCP) and [^{125}I]TID that results in increased labeling of the resting channel is somehow an artifact of photolabeling. Because barbiturates and TID bind to the same locus in the resting channel [8], we examined the effect of ketamine and TCP on [^{14}C]amobarbital binding, and in reciprocal fashion the effect of amobarbital on [^{3}H]TCP binding. As shown in Fig. 4, ketamine had virtually no effect on [^{14}C]amobarbital binding to the resting AChR, even at 200 μM, the highest concentration that we tested. The *S*(+)-ketamine enantiomer (Fig. 4) slightly inhibited [^{14}C]amobarbital binding. For instance, at 200 μM *S*(+)-ketamine specific binding is inhibited by ∼25%. Although there is a little maximal displacement, we infer the apparent K_i value for *S*(+)-ketamine (430 μM; $n_H = 0.32$; Table 1) in order to compare with the values from the other competing drugs.

Thienylcyclohexylpiperidine, like ketamine, only slightly inhibited [^{14}C]amobarbital binding to the resting AChR (Fig. 5A). For example, [^{14}C]amobarbital binding is reduced by ∼25% by 200 μM TCP. Although there is a little maximal displacement, we infer the apparent K_i value for TCP (5.1 mM; $n_H = 0.22$; Table 1) to compare with its true K_d value (0.83 μM; Arias, Trudell, Bayer, Hester, McCardy, and Blanton, in preparation). In reciprocal fashion, amobarbital inhibited [^{3}H]TCP

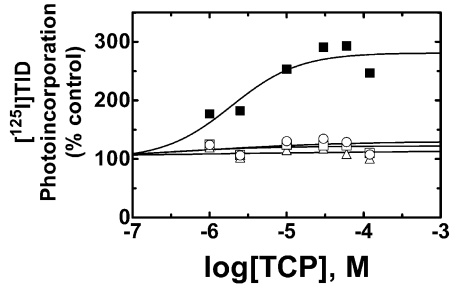

Fig. 3. TCP-induced potentiation of [^{125}I]TID photoincorporation into the AChR δ-subunit. AChR native membranes (0.2 μM) were equilibrated (1 h) with [^{125}I]TID (430 nM), in the presence of increasing concentrations of TCP (0.01–200 μM). The AChR membranes were photolabeled and the labeled subunits resolved by SDS–PAGE as described under Material and methods. The bands containing the α- (○), β- (□), γ- (△), and δ-subunit (■) were excised and the amount of ^{125}I cpm determined. Nonspecific binding was determined in the presence of 0.4 mM carb. The EC_{50} value for TCP potentiation of [^{125}I]TID photoincorporation into the δ-subunit was calculated by nonlinear least-squares fit (1.9 μM) and the result is reported in Table 1.

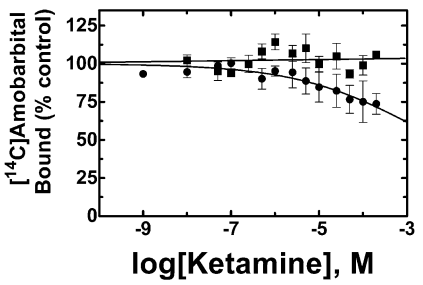

Fig. 4. Allosteric modulation of [^{14}C]amobarbital binding by ketamine. AChR native membranes (0.2 μM) were equilibrated (1 h) with [^{14}C]amobarbital (7.5 μM), in the presence of increasing concentrations (0.01–200 μM) of either a racemic mixture of ketamine (■) or *S*(+)-ketamine (●). AChR native membranes were then centrifuged and the radioactivity present in the pellet was determined by liquid scintillation counting as described under Materials and methods. Nonspecific binding was assessed in the presence of 200 μM amobarbital or 100 μM tetracaine. Each plot is the average of four different experiments. The IC_{50} value for the *S*(+)-ketamine enantiomer was calculated by nonlinear least-squares fit for a single binding site. The K_i value was calculated using this IC_{50} according to Eq. (1) and reported in Table 2.

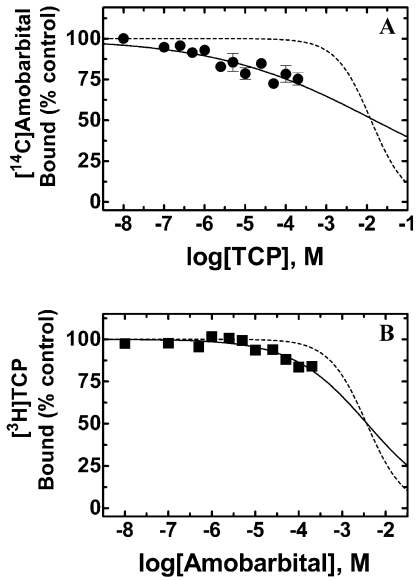

Fig. 5. Partial inhibition of [^{14}C]amobarbital binding by TCP (A) and of [^{3}H]TCP binding by amobarbital (B). AChR native membranes (0.2 μM) were equilibrated (1 h) with [^{14}C]amobarbital (7.5 μM) or [^{3}H]TCP (6.4 nM), in the presence of increasing concentrations (0.01–200 μM) of TCP or amobarbital, respectively. Each plot is the average of three different experiments. The IC_{50} value for either TCP or amobarbital was calculated by nonlinear least-squares fit (—). For the purpose of comparison, the nonlinear fit for a single binding site ($n_H = 1$) is also shown (– – –). The K_i for each drug was calculated using these IC_{50} values according to Eq. (1) and summarized in Table 1.

binding (Fig. 5B) with very low potency. Again, although there is a little maximal displacement, we infer the apparent K_i value for amobarbital (3.7 mM; $n_H = 0.51$; Table 1) to compare with its true K_d value [3.7 μM; [8]]. The extremely weak inhibition constants for TCP and amobarbital are several orders of magnitude higher than their respective equilibrium binding constants. This fact coupled with n_H values that are significantly different than one, strongly suggest that both *S*(+)-ketamine- or TCP-induced inhibition of [^{14}C]amobarbital binding, as well as amobarbital-induced inhibition of [^{3}H]TCP binding, are mediated by an allosteric mechanism and not by direct competition. In other words, it is unlikely that the binding site for ketamine or TCP spatially overlaps the barbiturate locus. The fact that TCP (or ketamine) positively modulates [^{125}I]TID photoincorporation in an allosteric manner (Figs. 1–3), while they barely affect [^{14}C]amobarbital binding (Figs. 4 and 5A), being that TID and amobarbital bind to the same site in the resting AChR ion channel [8], suggests several possibilities: (i) the molecular determinants of TID and barbiturate binding are similar but not identical, (ii) ketamine may not significantly affect the overall binding affinity of either TID or barbiturate but rather affect the binding orientation of each NCA which has a more selective effect on the efficiency of [^{125}I]TID photoincorporation. The fact that there is no discernible change in the [^{125}I]TID subunit labeling pattern in the presence of ketamine (see Figs. 1 and 2) suggests that, for the latter possibility, the effect of ketamine on the orientation of TID must be rather subtle.

Inhibition of [^{3}H]tetracaine binding by ketamine and TCP, and of [^{3}H]TCP binding by ketamine and tetracaine in the resting AChR

To more fully examine the molecular determinants of the ketamine (or TCP)-binding site in the resting AChR, we next determined the effect of ketamine and TCP on [^{3}H]tetracaine binding, and in reciprocal fashion the effect of tetracaine and ketamine on [^{3}H]TCP binding. In the absence of agonist, TCP, ketamine or *S*(+)-ketamine each completely eliminated specific [^{3}H]tetracaine binding to the resting AChR in a concentration-dependent fashion (Figs. 6A and B; 7A). For example, at high concentrations, TCP inhibited at least 98% of specifically bound [^{3}H]tetracaine (Fig. 7A). From nonlinear least-squares analysis of the binding data the following potencies were determined, in rank order (Table 2): TCP ($K_i = 2.0$ μM) > *S*(+)-ketamine ($K_i = 19.9$ μM) ~ racemic ketamine ($K_i = 20.9$ μM). In reciprocal fashion, tetracaine (Fig. 7B) and both ketamine and *S*(+)-ketamine (Fig. 8A) completely displaced specific [^{3}H]TCP binding to the resting AChR in the following rank order (Table 2): tetracaine ($K_i = 0.74$ μM) > racemic ketamine ($K_i = 16.5$ μM) ~ *S*(+)-ketamine ($K_i = 18.2$ μM). The fact that each of these NCAs completely displaces the binding of the other and with estimated n_H values near unity indicates that these interactions appear to be formally competitive and are mediated by a steric mechanism. Along these lines, it is significant that the K_i value for tetracaine inhibition of [^{3}H]TCP binding (0.74 μM; Table 2) is very close to the reported K_d value for tetracaine binding to the resting receptor [$K_d \sim 0.5$ μM; [5]]. With respect to the ketamine binding site, it is noteworthy that both the racemic mixture of ketamine (*R*(−) and *S*(+) enantiomers) or its *S*(+) enantiomer inhibited either [^{3}H]tetracaine (Fig. 6A) or [^{3}H]TCP (Fig. 8A) binding with nearly identical potencies, which suggests that the ketamine binding site is not stereoselective. This is in apparent contradiction with the results from [^{125}I]TID experiments (Fig. 1B) where the effect elicited by *S*(+)-ketamine on the [^{125}I]TID photoincorporation to both δ- and γ-subunits was slightly higher than the effect elicited by ketamine (see Table 1). One possible explanation is that *S*(+)-ketamine affects the binding orientation of [^{125}I]TID in a higher extent than ketamine.

Next, to further establish that the ketamine-induced inhibition of [^{3}H]tetracaine binding is mediated by a competitive (steric) mechanism, we assessed the inhibition of [^{3}H]tetracaine binding by ketamine using

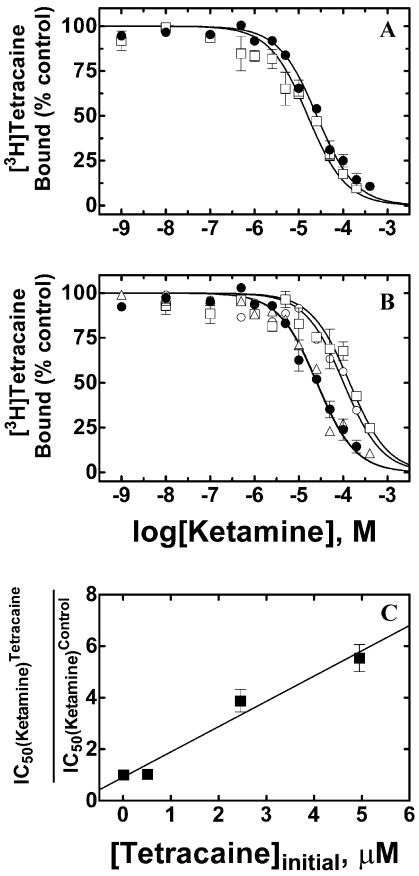

Fig. 6. Ketamine-induced inhibition of [^{3}H]tetracaine binding to the resting AChR. (A) AChR native membranes (0.2 μM) were equilibrated (1 h) with [^{3}H]tetracaine (6.9 nM) in the presence of increasing concentrations (0.01–200 μM) of racemic ketamine (●) or *S*(+)-ketamine (□). The AChR membranes were centrifuged and the radioactivity present in the pellets was measured as described under Materials and methods. Nonspecific binding was determined in the presence of 100 μM tetracaine. Each plot is the average of three different experiments. The IC_{50} value for ketamine (or *S*(+)-ketamine) was calculated by nonlinear least-squares fit for a single binding site. The K_i values were calculated using these IC_{50} values according to Eq. (1) and reported in Table 2. (B) AChR native membranes (0.2 μM) were equilibrated (1 h) with [^{3}H]tetracaine at initial concentrations of 6.9 (●); 504 (Δ); 2455 (○); and 4970 nM (□), respectively. (C) The apparent IC_{50} values were plotted as $[IC_{50}(\text{ketamine})^{\text{tetracaine}}/IC_{50}(\text{ketamine})^{\text{control}}]$ versus $[\text{tetracaine}]_{\text{initial}}$, following a Schild-type analysis [29]. From the linear regression a slope of 0.98 ± 0.10 and a correlation coefficient (r^2) of 0.908 were obtained.

increasing initial concentrations of [^{3}H]tetracaine (from 6.9 to 4970 nM; Fig. 6B). From these competition curves we calculated the apparent IC_{50} values, and by using a Shild-type analysis [29], we observed a linear relationship (Fig. 6C). A linear relationship supports the conclusion that ketamine inhibits [^{3}H]tetracaine binding in a competitive manner, by a steric mechanism. Nevertheless, a very strong allosteric inhibitory interaction between ketamine and tetracaine cannot be ruled out. All the data are in agreement, indicating a binding site for ketamine (or TCP) overlapping, at least partially, with the tetracaine locus.

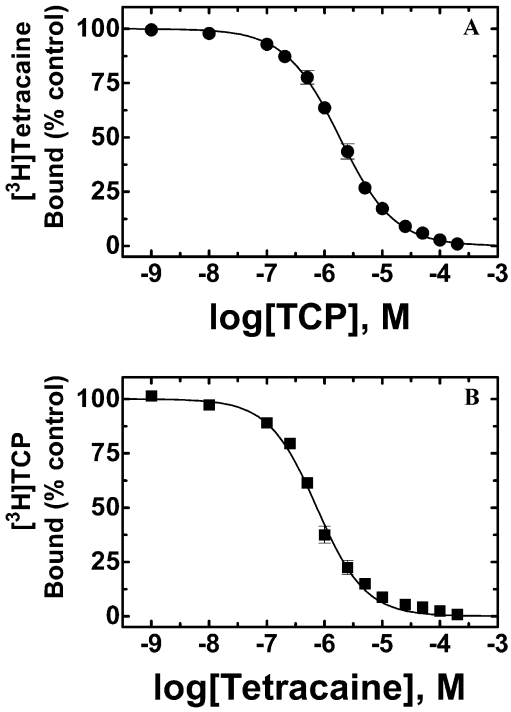

Fig. 7. Inhibition of [^{3}H]tetracaine binding by TCP (A) and of [^{3}H]TCP binding by tetracaine (B). AChR native membranes (0.2 μM) were equilibrated (1 h) with [^{3}H]tetracaine (6.9 nM) or [^{3}H]TCP (6.4 nM) in the presence of increasing concentrations (0.01–200 μM) of TCP (●) or tetracaine (■), respectively, in the absence of carb (resting state). The AChR membranes were centrifuged and the radioactivity present in the pellets was determined as described under Materials and methods. Nonspecific binding was assessed in the presence of 100 μM tetracaine. Each plot is the average of three different experiments. The IC_{50} value for TCP or tetracaine was calculated by nonlinear least-squares fit for a single binding site. The K_i for each drug was calculated using these IC_{50} values according to Eq. (1) and reported in Table 2.

Ketamine-induced inhibition of [^{3}H]TCP binding to the desensitized AChR

Lastly we wished to determine whether ketamine binds to the TCP binding site on the desensitized AChR. The effect of the racemic mixture of ketamine or its *S*(+) enantiomer on [^{3}H]TCP binding to the AChR in the presence of carb (desensitized state) was examined (Fig. 8B). Both ketamine and *S*(+)-ketamine displaced specific [^{3}H]TCP binding to the desensitized AChR in a concentration-dependent fashion, albeit with slightly increased potencies relative to those observed for the resting AChR (Table 2). For example, at high concentrations of ketamine greater than 95% of [^{3}H]TCP binding is inhibited and the observed K_is for the racemic ketamine mixture and *S*(+)-ketamine were 13.1 ± 1.8 and 15.4 ± 2.3 μM, respectively. From these results and considering that the n_H values are close to one (Table 2), we can conclude that in the desensitized AChR, the binding site for ketamine overlaps with the TCP locus in a nonstereoselective fashion.

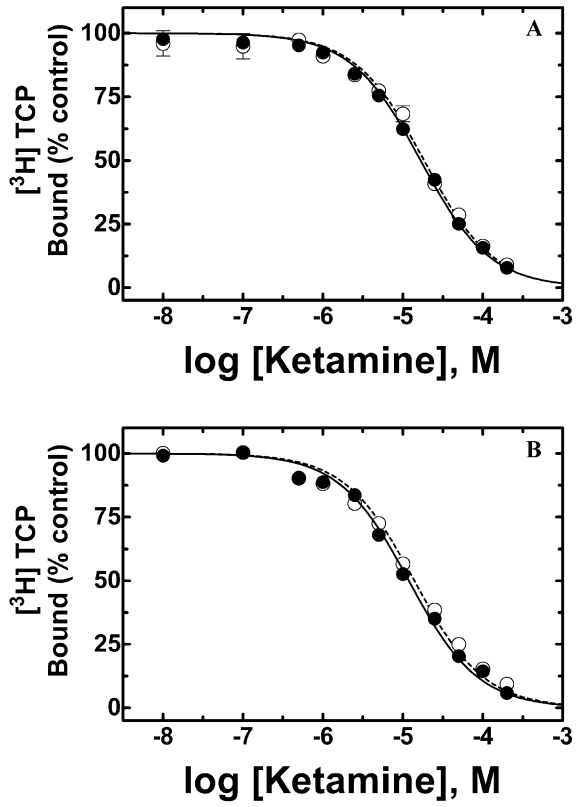

Fig. 8. Ketamine-induced inhibition of [^{3}H]TCP binding to the resting (A) and desensitized (B) AChR. AChR native membranes (0.2 μM) were equilibrated (1 h) with [^{3}H]TCP (6.4 nM), in the absence (A) or presence (B) of 200 μM carb, and increasing concentrations (0.01–200 μM) of a racemic mixture of ketamine (●) or *S*(+)-ketamine (○), respectively. The AChR membranes were centrifuged and the radioactivity present in the pellets was measured as described under Materials and methods. Nonspecific binding was determined in the presence of 100 μM tetracaine (resting experiments) or 200 μM meproadifen (desensitized experiments). Each plot is the average of three different experiments. The IC_{50} value for ketamine and *S*(+)-ketamine was calculated by nonlinear least-squares fit for a single binding site. The K_i for ketamine and *S*(+)-ketamine was calculated using these IC_{50} values according to Eq. (1) and summarized in Table 2.

Discussion

In order to characterize and potentially localize the binding site for the dissociative anesthetics ketamine and TCP in the resting AChR, we have taken into consideration previous studies that have established the binding sites for the well-known NCAs TID [9,10], tetracaine [11], and barbiturates [8] in the resting AChR channel. In the present study, we examined the effect of ketamine and TCP on the pattern of photolabeling of [^{125}I]TID and of [^{14}C]amobarbital, [^{3}H]TCP, and [^{3}H]tetracaine binding, in the resting AChR. In reciprocal fashion, the effect of amobarbital, ketamine, and tetracaine on [^{3}H]TCP binding to the resting receptor was examined. Our results yielded what appear to be conflicting conclusions: a mutually exclusive interaction between ketamine (or TCP, barbiturate, and TID) and tetracaine, but an allosteric interaction between ketamine (or TCP) and TID (or barbiturates). More specifically:

(i) Both ketamine and TCP increased the extent (i.e., potentiated) of [^{125}I]TID photoincoporation into each AChR subunit. Importantly, both the pattern of [^{125}I]TID photoincorporation into receptor subunits (e.g., 4-fold greater labeling of the γ-subunit relative to the α-, β-, δ-subunits is maintained; Fig. 1) and the proteolytic mapping results (within the α-subunit, only labeling of αV8–20 is affected; Fig. 2) indicate that the change in [^{125}I]TID incorporation reflects a specific change in labeling of the resting channel. Along these lines, previous photolabeling experiments have demonstrated that PCP, a close structural analog of TCP, also potentiates [^{125}I]TID photoincoporation into the AChR δ-subunit [14] and the effect of PCP is to subtly shift the orientation of the TID molecule within its resting channel binding site [13]. We conclude from these results that ketamine and TCP (and PCP) interact allosterically with TID, and that neither ketamine, TCP, or PCP bind at the level of M2–9/M2–13, the established binding locus for TID within the resting AChR channel (see also [13]). Consistent with this conclusion, mutations at β2Val^{253} (M2–13) do not produce any effect on ketamine-induced inhibition of α4β2 neuronal-type AChR channels [21].

(ii) Ketamine does not produce any effect on [^{14}C]amobarbital binding and the *S*(+) enantiomer of ketamine alone and TCP only slightly inhibit [^{14}C]amobarbital binding and with n_H values that deviate significantly from unity ($n_H = 0.22$–0.32; Table 1). Reciprocally, amobarbital inhibits [^{3}H]TCP binding only marginally and again with a n_H value that is far from unity (Table 1). These results are consistent with an allosteric interaction, if any, between *S*(+)-ketamine (or TCP) and amobarbital, and that ketamine and TCP do not bind at the barbiturate binding locus within the resting AChR channel. Since the barbiturate binding site overlaps that for TID [8], these results are in agreement with the earlier conclusion indicating an allosteric interaction between ketamine (or TCP) and TID, and that the binding site(s) for these dissociative anesthetics does not overlap that for TID.

(iii) Both ketamine and TCP completely inhibit [^{3}H]tetracaine binding to the resting AChR and the results strongly suggest a competitive, mutually exclusive interaction (e.g., Fig. 6). Along these same lines, a simple competitive interaction between PCP and [^{3}H]tetracaine binding to the resting AChR has been observed [5]. In reciprocal fashion, our experiments indicate that tetracaine inhibits [^{3}H]TCP binding by a mutually exclusive mechanism (Fig. 7), and that ketamine and TCP interact competitively (Fig. 8). This latter result is in agreement with previous experiments showing that ketamine inhibits [^{3}H]PCP binding to the *Torpedo* AChR in both resting and desensitized conformational states

[17,22]. Collectively, the evidence demonstrates that the dissociative anesthetics ketamine, TCP, and PCP bind to a single or overlapping sites on the resting AChR, and suggest that the ketamine (or TCP) binding site spatially overlap the tetracaine site, which is located approximately between positions M2–16/17 and M2–5 [13] in the resting AChR channel. Considering that the high-affinity barbiturate binding site overlaps the site for tetracaine and TID [8], a full overlapping between the tetracaine and the ketamine (or TCP) site should also include the barbiturate (or TID) binding site, and this was not observed in our experiments. Thus, we can conclude that there is only partial spatial overlap between the TCP (or ketamine) molecule and the tetracaine molecule when each is bound to their respective sites in the resting channel.

These apparently conflicting conclusions, e.g., mutually exclusive action between ketamine (or TCP) and tetracaine and between TID (or barbiturates) and tetracaine, but allosteric interaction between ketamine (or TCP) and TID (or barbiturates), can be reconciled by proposing the following: The extended conformation of the tetracaine molecule is longer than either the TID or the barbiturate molecule (see Fig. 9) [11]; therefore, there are at least two possibilities of how the ketamine (or TCP) molecule may be accommodated within the resting ion channel in order to partially overlap with the tetracaine binding site but allosterically interact with the TID (or barbiturate) locus. One possibility is that the ketamine (or the TCP) binding site is located closer to the carboxyl terminal end of the M2 transmembrane domain (more extracellular, between M2–13 and M2–20; see Fig. 9). Based on several lines of reasoning and the pattern of [^{3}H]tetracaine photoincorporation into M2-containing amino acids, Gallagher and Cohen [11] positioned the tetracaine molecule within the resting AChR channel such that the dimethylaminoethyl group is in approximate register with M2–5 whereas its *N*-butyl group is aligned with hydrophobic residues toward the carboxyl-terminus of the M2 segment (e.g., M2–16/17). As is evident in Fig. 9, because the tetracaine molecule extends above M2–13, it therefore spatially overlaps the ketamine (or TCP) molecule, and this accounts for the competitive interaction between ketamine (or TCP) and tetracaine. On the other hand, the model in Fig. 9 also illustrates how both ketamine (or TCP) and TID (or amobarbital) may bind simultaneously within the resting channel. The binding effects observed for TID (or amobarbital) and ketamine (or TCP and PCP) may result from either local perturbations in the structure of the channel or perhaps allosteric stabilization of an intermediate conformational state as was concluded for the effects of PCP on the resting AChR (see [14]). An alternative possibility is that the ketamine (or TCP) site is positioned in closer proximity to the amino-terminal end of the M2 transmembrane domain (more cytoplasmic, below M2–9). While we cannot exclude this possibility we find it much less likely given the fact that ketamine, a two-ring aromatic secondary amine, and TCP, a three-ring aromatic tertiary amine, are either approximately equal or significantly larger in size than TID, while M2–9 is the most cytoplasmically located amino acid that is photolabeled by [^{125}I]TID. Secondly, the fact that a rather bulky NCA such as chlorpromazine may be accommodated within the channel between M2–6 and M2–9 solely in the desensitized state (reviewed in [3,4]) suggests that the size of this portion of the channel in the resting state is smaller than in the desensitized state.

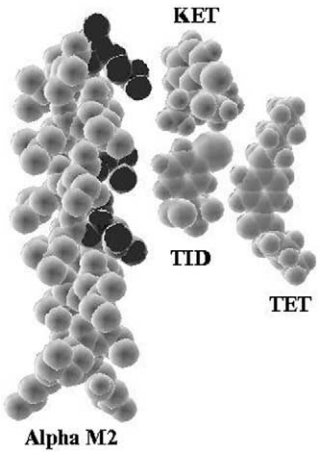

Fig. 9. Model of ketamine, TID, and tetracaine complexed with the resting AChR ion channel. Space-filling, α-helical model of the M2 segment of the α-subunit and models at the same scale of ketamine, tetracaine, and TID were constructed using the molecular modeling software Sybyl (Tripos). The positioning of TID and tetracaine relative to the αM2 segment is based on photoaffinity labeling studies and the identified labeled amino acids on each M2 segment [9,11]. The proposed positioning of the ketamine molecule is based on radioligand binding and photolabeling experiments and accounts for the competitive interaction between ketamine and tetracaine and the allosteric interaction between ketamine and TID. For reference, αM2 residues at position 9, 13 (TID binding locus), and 20 are shaded.

Ketamine competitively inhibits [^{3}H]TCP binding to the receptor in both the resting and the desensitized conformation (Fig. 8). Similar results were observed for ketamine displacement of [^{3}H]PCP binding [17,22]. Photoaffinity labeling experiments using [^{3}H]azido-PCP have mapped the high-affinity PCP site on both the resting and the desensitized AChR to a proteolytic fragment containing the transmembrane segments M1–M2–M3 [32]. In the muscle-type AChR open channel, the PCP binding site is believed to be located between the conserved ring of leucine residues (M2–9) and the more cytoplasmic ring of serine residues (M2–6) [33,34] (reviewed in [3,4]) However, a more complex process involving nonluminal inhibitory and regulatory sites for PCP has been hypothesized as well [34]. Given the competitive nature of the interaction between ketamine

and [^{3}H]TCP for binding to the desensitized AChR (Fig. 8; Table 2) and the structural similitude among ketamine, TCP, and PCP it is likely that these dissociative anesthetics, like for the resting AChR channel, bind to a single or overlapping binding site(s) in either the desensitized or the open channel.

Finally, it is also noteworthy that ketamine inhibited [^{3}H]TCP binding to the resting and desensitized AChR in an apparently nonstereoselective manner (Fig. 8; Table 2). This constrasts with a nearly 4-fold difference in potency between the two stereoisomers [$S(+) > R(-)$] for inhibition of ganglionic neuronal-type AChRs [18]. We are currently investigating whether this difference results from stereoselective interaction of ketamine with the channel in the open state or sequence differences between *Torpedo* muscle-type and neuronal-type AChRs.

Acknowledgments

We thank Dr. Jay Ponder (Washington University School of Medicine, St. Louis, MO) for use of his computer workstation, molecular graphics software, and invaluable assistance. This research was supported in part by National Institutes of Health Grant R29-NS35786 (M.P.B.).

References

[1] H.R. Arias, Neurochem. Int. 36 (2000) 595–645.
[2] P.-J. Corringer, N. Le Novére, J.-P. Changeux, Annu. Rev. Pharmacol. Toxicol. 40 (2000) 431–458.
[3] H.R. Arias, in: R.B. Raffa (Ed.), Drug-Receptor Thermodynamics: Introduction and Applications, Wiley, USA, 2001, pp. 293–358.
[4] H.R. Arias, Biochim. Biophys. Acta 1376 (1998) 173–220.
[5] R.E. Middleton, N.P. Strnad, J.B. Cohen, Mol. Pharmacol. 56 (1999) 290–299.
[6] B.H. White, S. Howard, S.G. Cohen, J.B. Cohen, J. Biol. Chem. 266 (1991) 21595–21607.
[7] D.C. Chiara, M.A. Kloczewiak, G.H. Addona, J.-A. Yu, J.B. Cohen, K.W. Miller, Biochemistry 40 (2001) 296–304.
[8] H.R. Arias, E.A. McCardy, M.J. Gallagher, M.P. Blanton, Mol. Pharmacol. 60 (2001) 497–506.
[9] B.H. White, J.B. Cohen, J. Biol. Chem. 267 (1992) 15770–15783.
[10] M.P. Blanton, E.A. McCardy, M.J. Gallagher, J. Biol. Chem. 275 (2000) 3469–3478.
[11] M.J. Gallagher, J.B. Cohen, Mol. Pharmacol. 56 (1999) 300–307.
[12] T. Heidmann, R.E. Oswald, J.-P. Changeux, Biochemistry 22 (1983) 3112–3127.
[13] M.J. Gallagher, D.C. Chiara, J.B. Cohen, Mol. Pharmacol. 59 (2001) 1514–1522.
[14] S.E. Ryan, M.P. Blanton, J.E. Baenziger, J. Biol. Chem. 276 (2001) 4796–4803.
[15] M.A. Maleque, J.E. Warnick, E.X. Albuquerque, J. Pharmacol. Exp. Ther. 219 (1981) 638–645.
[16] M. Scheller, J. Bufler, I. Hertle, H.J. Schneck, C. Franke, E. Kochs, Anesth. Analg. 83 (1996) 830–836.
[17] R.L. Volle, K.A. Alkadhi, D.D. Branisteanu, L.S. Reynolds, P.M. Epstein, H. Smilowitz, J.J. Lambert, E.G. Henderson, J. Pharm. Exp. Ther. 221 (1982) 570–576.
[18] P. Friederich, A. Dybek, B. Urban, Anesthesiology 93 (2000) 818–824.
[19] R. Furuya, K. Oka, I. Watanabe, Y. Kamiya, H. Itoh, T. Andoh, Anesth. Analg. 88 (1999) 174–180.
[20] T. Yamakura, L.E. Chavez-Noriega, A. Harris, Anesthesiology 92 (2000) 1144–1153.
[21] T. Yamakura, C. Borghese, A. Harris, J. Biol. Chem. 275 (2000) 40879–40886.
[22] R.S. Aronstam, L. Narayanan, D.A. Wenger, Eur. J. Pharmacol. 78 (1982) 367–370.
[23] E.J. Katz, V.I. Cortes, M.E. Eldefrawi, A.T. Eldefrawi, Toxicol. Appl. Pharmacol. 146 (1997) 227–236.
[24] O.R. Pagán, V.A. Eterović, M. Garcia, D. Vergne, C.M. Basilio, A.D. Rodríguez, R.M. Hann, Biochemistry 40 (2001) 11121–11130.
[25] S.E. Pedersen, E.B. Dreyer, J.B. Cohen, J. Biol. Chem. 261 (1986) 13735–13743.
[26] D.W. Cleveland, S.G. Fischer, M.W. Kirschner, U.K. Laemmli, J. Biol. Chem. 252 (1977) 1101–1106.
[27] M.P. Blanton, E.A. McCardy, A. Huggins, D. Parikh, Biochemistry 37 (1998) 407–414.
[28] Y.C. Cheng, W.H. Prusoff, Biochem. Pharmacol. 22 (1973) 3099–3108.
[29] H.O. Schild, Br. J. Pharmacol. 4 (1949) 277–280.
[30] M.P. Blanton, J.B. Cohen, Biochemistry 31 (1992) 3738–3750.
[31] M.P. Blanton, J.B. Cohen, Biochemistry 33 (1994) 2859–2872.
[32] R. Mosckovitz, R. Haring, J.M. Gershoni, Y. Kloog, M. Sokolovsky, Biochem. Biophys. Res. Commun. 145 (1987) 810–816.
[33] V.A. Eterovi, R. Lu, A.E. Eakin, A.D. Rodríguez, P.A. Ferchmin, Cell. Mol. Neurobiol. 19 (1999) 745–757.
[34] M.J. Eaton, C.G. Labarca, V.A. Eterović, J. Neurosci. Res. 61 (2000) 44–51.